SF2A 2010
S. Boissier, M. Heydari-Malayeri, R. Samadi and D. Valls-Gabaud (eds)

SED FITTING OF NEARBY GALAXIES IN THE HERSCHEL REFERENCE SURVEY

L. Ciesla[1], A. Boselli[1], V. Buat[1], L. Cortese[2], R. Auld[2], M. Baes[2], G.J. Bendo[2], S. Bianchi[2], J. Bock[2], D.J. Bomans[2], M. Bradford[2], N. Castro-Rodriguez[2], P. Chanial[2], S. Charlot[2], M. Clemens[2], D. Clements[2], E. Corbell[2], A. Cooray[2], D. Cormie[2], A. Dariush[2], J. Davies[2], I. De Looze[2], S. di Serego Alighieri[2], E. Dwek[2], S. Eales2, D. Elbaz[2], D. Fadda[2], J. Fritz[2], M. Galametz[2], F. Galliano[2], D.A. Garcia-Appadoo[2], G. Gavazzi[2], W. Gear[2], C. Giovanardi[2], J. Glenn[2], H. Gomez[2], M. Griffin[2], M. Grossi[2], S. Hony[2], T.M. Hughes[2], L. Hunt[2], K. Isaak[2], A. Jones[2], L. Levenson[2], N. Lu[2], S.C. Madden[2], B. O'Halloran[2] , K. Okumura[2], S. Oliver[2], M. Page[2], P. Panuzzo[2], A. Papageorgiou[2], T. Parkin[2], I. Perez-Fournon[2], D. Pierini[2], M. Pohlen[2], N. Rangwala[2], E. Rigby[2], H. Roussel[2], A. Rykala[2], S. Sabatini[2], N. Sacchi[2], M. Sauvage[2], B. Schulz[2], M. Schirm[2], M.W.L. Smith[2], L. Spinoglio[2], J. Stevens[2], S. Sundar[2], M. Symeonidis[2], M. Trichas[2], M. Vaccari[2], J. Verstappen[2], L. Vigroux[2], C. Vlahakis[2], C. Wilson[2], H. Wozniak[2], G. Wright[2], E.M. Xilouris[2], W. Zeilinger[2] and S. Zibetti [2]

Abstract. We compute UV to radio continuum spectral energy distributions of 51 nearby galaxies recently observed with SPIRE onboard Herschel and present infrared colours (in the $25 - 500\mu$m spectral range). SPIRE data of normal galaxies are well reproduced with a modified black body (β=2) of temperature $T\simeq$ 20 K. In ellipticals hosting a radio galaxy, the far-infrared (FIR) emission is dominated by the synchrotron nuclear emission. The colour temperature of the cold dust is higher in quiescent E-S0a than in star-forming systems probably because of the different nature of their dust heating sources (evolved stellar populations, X-ray, fast electrons) and dust grain properties.

Keywords: Galaxies: ISM; spiral; elliptical and lenticular; Infrared: galaxies

1 Introduction

By constructing the spectral energy distribution (SED) of any extragalactic source, its energetic output can be determined. The stellar component emits from the UV to near-infrared (NIR) domain, young and massive stars dominating the UV and old stars the NIR. Dust, produced by the aggregation of metals injected into the interstellar medium (ISM) by massive stars through stellar winds and supernovae, efficiently absorbs the stellar light, in particular that at short wavelengths, and re-emits it in the infrared domain (5μm-1mm). At longer wavelengths, the emission of normal galaxies is generally dominated by the loss of energy of relativistic electrons accelerated in supernovae remnants (Lequeux 1971; Kennicutt 1983) (synchrotron emission). SEDs are crucial for quantifying dust extinction and reconstructing the intrinsic distribution of the different stellar populations within galaxies. In particular, the importance of the infrared domain explored by Herschel resides in the dust that, by means of the absorption and scattering of UV, optical and NIR photons, modifies the stellar spectra of galaxies. The interpretation of the infrared SEDs of normal galaxies has already been the subject of several studies (e.g. Dale et al. 2007; Chary & Elbaz 2001) even within the Virgo cluster region (Boselli et al. 1998; 2003) which were limited in the infrared domain to $\lambda \leq 170$ μm (domain covered by ISO or Spitzer) With the Herschel data, we can extend to the sub-mm domain ($\lambda \leq 500$ μm) where the emission is dominated by the coldest dust component. This domain is crucial for determining galaxy properties such as the total mass of dust, and an accurate total infrared luminosity. Galaxies analysed in this work were observed

[1] Laboratoire d'Astrophysique de Marseille, UMR6110 CNRS, 38 rue F.Joliot-Curie, F-13388 Marseille France
[2] Members of the Herschel/SPIRE guaranteed time Extragalactic Working Group (SAG2)

during the Herschel (Pilbratt et al. 2010) SPIRE (Griffin et al. 2010) science demonstration phase mainly as part of the Herschel Reference Survey (HRS), a guaranteed time key project designed to observe with SPIRE a volume-limited, K-band-selected, complete sample of nearby galaxies (Boselli et al. 2010), and the Herschel Virgo Cluster Survey (HeViCS), an open time key project focused on covering 60 sq.deg. of the Virgo cluster with PACS and SPIRE (Davies et al. 2010). The results of this analysis have been presented in Boselli et al. (2010b).

2 Far infrared colours

We determine the IR colours of the galaxies in order to quantify their spectral properties combining SPIRE and IRAS flux densities (Fig. 1). These colour diagrams indicate that in star-forming galaxies the flux density ratios $f60/f500$, $f25/f250$, or $f100/f250$ are strongly correlated with the generally used IRAS colour index $f60/f100$ (panels a, b and c). However, the dynamic range covered by $f60/f500$ is a factor of about 30 larger than that covered by the $f60/f100$ flux density ratio. The colour index is thus a powerful tracer of the average temperature of the dust component. Starburst galaxies, generally defined to have $f60/f100 > 0.5$ (Rowan-Robinson & Crawford 1989), show $f60/f500$ spanning from ~ 3 to ~ 30 and Sa-Sb have $f60/f500$ colours generally colder than Sbc-Scd, Sd, Im, BCD, and Irr. Early-types with a synchrotron-dominated IR emission (M87, M84) are well separated in all colour diagrams with respect to the other dust-dominated E-S0a. Therefore, we can use colour diagrams in order to identify and discriminate radio galaxies from the remaining early-types. The remaining early-types have colour indices indicating that the cold dust temperature is higher than in star-forming systems.
Figure 1 also shows that, despite possible uncertainties in the absolute flux calibration (15 %), the empirical SEDs of Dale & Helou (2002), Chary & Elbaz (2001), and Boselli et al. (2003), cover only qualitatively the wide range of infrared colours observed in our sample (even excluding the radio galaxies M87 and M84), underpredict the $f250/f350$ ratio for a given $f100/f250$ ratio (d), and do not reproduce the coldest colour temperatures observed in the diagram $f350/f500$ versus $f250/f350$ (f).

3 Spectral Energy Distribution

As a representative example of the target galaxies, we show the SED of two late-type galaxies (Fig2), M100 (NGC4321) and NGC4438, and two ellipticals (Fig3), M87 (NGC486) and M86 (NGC4406). The SED has been computed by combining data available in the literature. We match the 100μm IRAS data with a modified black body (β=2) of temperature $T \simeq 20$ K (magenta dashed line) and the radio data with a power law. Despite their very different morphology (M100 is a normal spiral galaxy while NGC4438 is a strongly interacting system), these two objects have quite similar SEDs. Contrarily, the galaxies M87 and M86 are both bright ellipticals but characterized by very different SEDs. In M87, the submilimeter emission detected by Herschel is due to synchrotron (Baes et al. 2010), while in M86 it is due to the cold dust nearbly falling into the galaxy after its interaction with nearby companions (Gomez et al. 2010). These different SEDs for galaxies of the same morphological type clearly explain why galaxies of a given type have so different infrared colours.

4 Conclusions

The infrared colour index $f60/f500$ is more capable of detecting a starburst than $f60/f100$ due to a larger dynamical range. Normal galaxies show a gradual increase in their dust temperature along the Hubble sequence, from Sa to Sc-Im-BCD with the exception of E-S0a, where the dust temperature is higher than in star-forming systems probably because of the different nature of their dust heating sources. SPIRE colours can be used to discriminate thermal from synchrotron emission in radio galaxies. SED of radio galaxies clearly show the far-infrared dominated by the synchrotron emission. In normal galaxies, the modified black body seems to well reproduce the SPIRE data but it has to be detailed with a proper fit using the CIGALE code (Code Investigating GALaxy Emission, Noll et al. 2009).

References

Baes, M. et al. 2010, ApJ, 652, 283
Bendo, G. et al. 2010, A&A, 518, L65

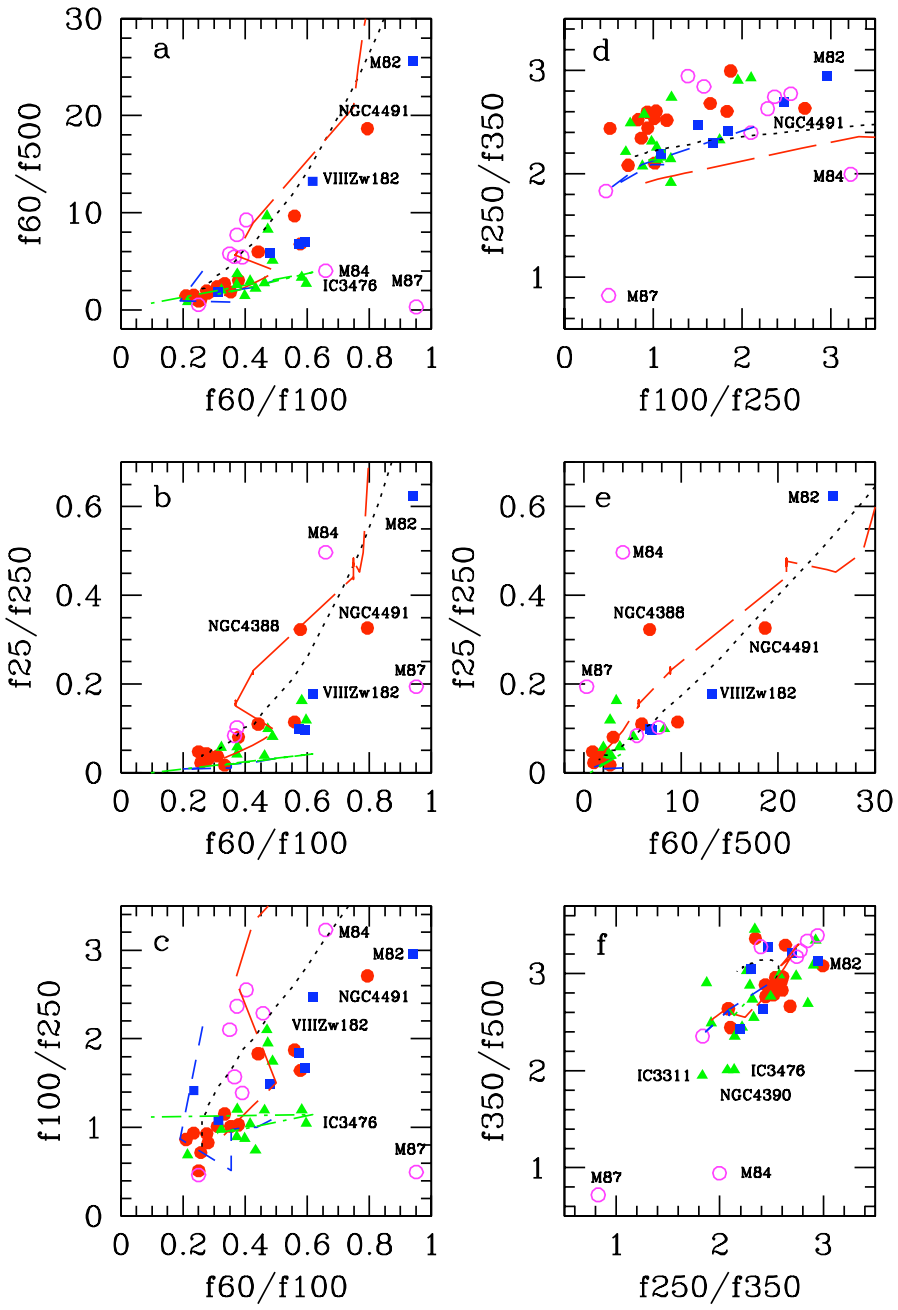

Fig. 1. The infrared colours of our targets. Galaxies are coded according to their morphological type: magenta empty circles for E-S0a, red filled circles for Sa-Sb, green triangles for Sbc- Scd, blue squares for Sd, Im, BCD, and Irr galaxies. The black dotted line indicates the colour expected from the Dale & Helou (2002) empirical SED, the red long-dashed line those from Chary & Elbaz (2001), the blue-short dashed, and the green dashed-dotted line the colours of the morphology- and luminosity-dependent templates of Boselli et al. (2003).

Boselli, A. and Gavazzi, G. 2006, PASP, 118, 517
Boselli, A., Lequeux, J., Sauvage, M., et al. 1998, A&A, 335, 53
Boselli, A., Gavazzi, G., Donas, J., Scodeggio, M. 2001, AJ, 121, 753
Boselli, A., Gavazzi, G., Sanvito, G., 2003, A&A, 402, 37
Boselli, A., Cortese, L., Deharveng, JM., et al. 2005, ApJ, 629, L29
Boselli, A., Boissier, S., Cortese, L., Buat, V., Hughes, T., Gavazzi, G. 2009, ApJ, 706, 1527
Boselli, A., Eales, S., Cortese, L., et al. 2010, PASP, 122, 261

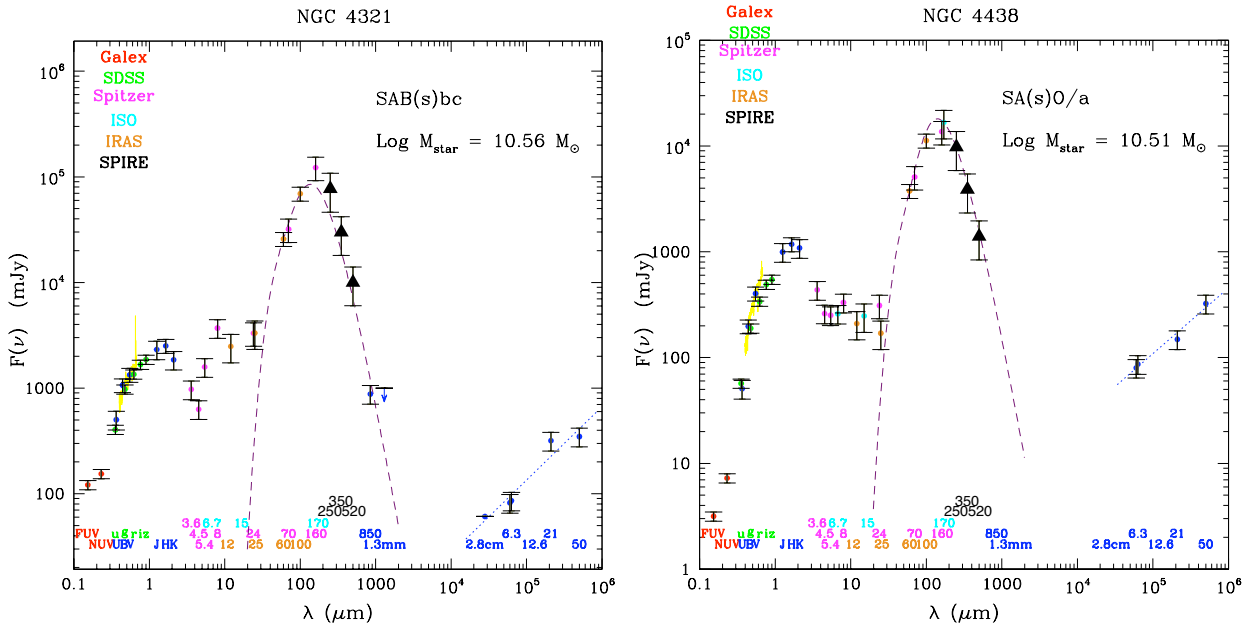

Fig. 2. The UV to radio SED of M100 (NGC4321) and NGC4438. Points are coloured according to the origin of the data. Black triangles are for Herschel-SPIRE data, red dots for GALEX data, green dots for SDSS data, magenta for Spitzer-IRAC and MIPS data, orange dots for IRAS data. Blue dots correspond to data from NED. The magenta dashed line shows a modified black body (β=2) of temperature $T\simeq$ 20 K matching the 100μm IRAS data, while the blue dotted-line indicates the radio power law spectrum due to synchrotron emission. We fit the radio data with a power law (blue dotted-line).

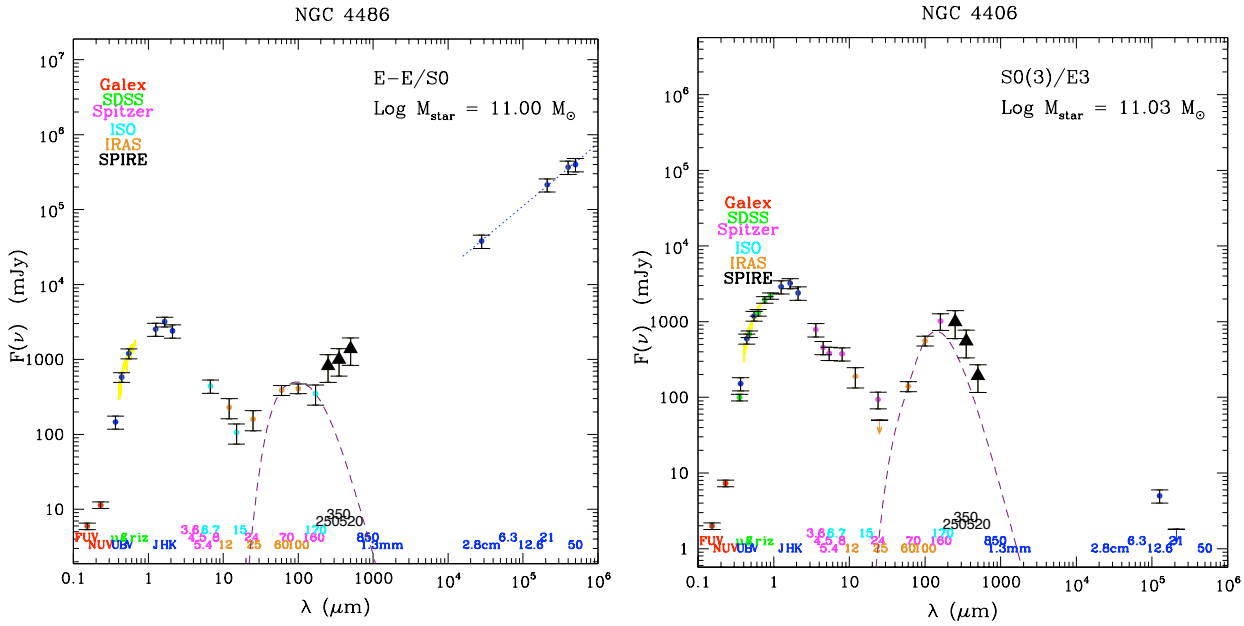

Fig. 3. The UV to radio SED of M87 (NGC4486) and M86 (NGC4406). Points are coloured according to the origin of the data. Black triangles are for Herschel-SPIRE data, red dots for GALEX data, green dots for SDSS data, magenta for Spitzer-IRAC and MIPS data, orange dots for IRAS data. Blue dots correspond to data from NED. The magenta dashed line shows a modified black body (β=2) of temperature $T\simeq$ 20 K matching the 100μm IRAS data while the blue dotted-line indicates the radio power law spectrum due to synchrotron emission.

Boselli, A., Ciesla, L., Buat, V., et al. 2010, A&A, 518, L61
Chary, R. and Elbaz, D. 2001, ApJ, 556, 562
Cortese, L., Davies, J., Pohlen, M., et al. 2010, A&A, 518, L63
Dale, D., Gil de Paz, A., Gordon, K., et al. 2007, ApJ, 655, 863
Dale, D. & Helou, G. 2002, ApJ, 576, 159
Davies, J., Baes, M., Bendo, G., et al. 2010, A&A, 518, L48
Draine, B. and Li, A. 2007, ApJ, 657, 810
Draine, B., Dale, D., Bendo, G., et al. 2007, ApJ, 663, 866
Galliano, F., Madden, S., Jones, A., Wilson, C., Bernard, J. 2005, A&A, 434, 867
Gavazzi, G., Boselli, A., Donati, A., Franzetti, P., Scodeggio, M. 2003, A&A, 400, 451
Gomez, H. et al. 2010, A&A, 518, L45
Griffin, M., et al. 2010, A&A, 518, L3
Kennicutt, R. 1983, A&A, 120, 219
Lequeux, J. 1971, A&A, 15, 42
Noll, S., Burgarella, D., Giovannoli, E., Buat, V. et al. 2009, A&A, 507, 1793
O'Connell, R. 1999, A&A, 37, 603
Pilbratt, G., et al. 2010, A&A, 518, L1
Pohlen, M., et al. 2010, A&A, 518, L72
Rowan-Robinson, M., Crawford, J. 1989, MNRAS, 238, 523
Swinyard, B., Ade, P, Baluteau, J.P., et al. 2010, A&A, 518, L4
Wolfire, M., Hollenbach, D., McKee, C., Tielens, A., Bakes, E. 1995, ApJ, 443, 152